Investigations on ring-shaped pumping distributions for the generation of beams with radial polarization in an Yb:YAG thin-disk laser

Tom Dietrich,* Martin Rumpel, Thomas Graf, and Marwan Abdou Ahmed

Institut fuer Strahlwerkzeuge (IFSW), University of Stuttgart, Pfaffenwaldring 43, 70569 Stuttgart, Germany

*tom.dietrich@ifsw.uni-stuttgart.de

Abstract: We present experimental investigations on the generation of radially polarized laser beams excited by a ring-shaped pump intensity distribution in combination with polarizing grating waveguide mirrors in an Yb:YAG thin-disk laser resonator. Hollow optical fiber components were implemented in the pump beam path to transform the commonly used flattop pumping distribution into a ring-shaped distribution. The investigation was focused on finding the optimum mode overlap between the ring-shaped pump spot and the excited first order Laguerre-Gaussian (LG_{01}) doughnut mode. The power, efficiency and polarization state of the emitted laser beam as well as the thermal behavior of the disk was compared to that obtained with a standard flattop pumping distribution. A maximum output power of 107 W with a high optical efficiency of 41.2% was achieved by implementing a 300 mm long specially manufactured hollow fiber into the pump beam path. Additionally it was found that at a pump power of 280 W the maximum temperature increase is about 21% below the one observed with standard homogeneous pumping.

OCIS codes: (140.3580) Lasers, solid-state; (140.5560) Pumping; (140.6810) Thermal effects; (050.1950) Diffraction gratings.

References and links

1. V. Niziev and A. Nesterov, "Influence of beam polarization on laser cutting efficiency," Appl. Phys. **32**(13), 1455–1461 (1999).
2. A. Weber, A. Michalowksi, M. A. Ahmed, V. Onuseit, V. Rominger, M. Kraus, and T. Graf, "Effects of radial and tangential polarization in laser material processing," Physics Procedia **12**(A), 21–30 (2011).
3. M. Kraus, M. A. Ahmed, A. Michalowksi, A. Voss, R. Weber, and T. Graf, "Microdrilling in steel using ultrashort pulsed laser beams with radial and azimuthal polarization," Opt. Express **18**(21), 22305–22313 (2010).
4. R. Dorn, S. Quabis, and G. Leuchs, "Focusing a radially polarized light beam to a significantly smaller spot size," arXiv preprint physics/0310007 (2003).
5. G. M. Lerman and U. Levy, "Tight focusing of spatially variant vector optical fields with elliptical symmetry of linear polarization," Opt. Lett. **32**(15), 2194–2196 (2007).
6. Z. Zhang, J. Pu, and X. Wang, "Tight focusing of radially and azimuthally polarized vortex beams through a uniaxial birefringent crystal," Appl. Opt. **47**(12), 1963–1967 (2008).
7. B. Tian and J. Pu, "Tight focusing of a double-ring-shaped, azimuthally polarized beam," Opt. Lett. **36**(11), 2014–2016 (2011).

#248339 Received 21 Aug 2015; revised 15 Sep 2015; accepted 15 Sep 2015; published 1 Oct 2015

8. T. A. Nieminen, N. R. Heckenberg, and H. Rubinsztein-Dunlop, "Forces in optical tweezers with radially and azimuthally polarized trapping beams," Opt. Lett. **33**(2), 122–124 (2008).
9. S. C. Tidwell, G. H. Kim, and W. D. Kimura, "Efficient radially polarized laser beam generation with a double interferometer," Appl. Opt. **32**(27), 5222–5229 (1993).
10. Z. Bomzon, G. Biener, V. Kleiner, and E. Hasman, "Radially and azimuthally polarized beams generated by space-variant dielectric subwavelength gratings," Opt. Lett. **27**(5), 285–287 (2007).
11. G. Machavariani, Y. Lumer, I. Moshe, A. Meir, and S. Jackel, "Efficient extracavity generation of radially and azimuthally polarized beams," Opt. Lett. **32**(11), 1468–1470 (2007).
12. M. A. Ahmed, M. Vogel, A. Voss, and T. Graf, "A 1-kW radially polarized thin-disk laser," in *Proceedings of IEEE Lasers and Electro-Optics and the European Quantum Electronics Conference* (IEEE, 2009), 10834335.
13. Z. Bomzon and E. Hasman, "The formation of laser beams with pure azimuthal or radial polarization," Appl. Phys. Lett. **77**(21), 3322–3324 (2000).
14. D. Delbeke, R. Baets, and P. Muys, "Polarization-selective beam splitter based on a highly efficient simple binary diffraction grating," Appl. Phys. Lett. **77**(33), 6157–6165 (2004).
15. M. Endo, "Azimuthally polarized 1 kW CO 2 laser with a triple-axicon retroreflector optical resonator," Opt. Lett. **33**(15), 1771–1773 (2008).
16. Y. Kozawa, S. Sato, T. Sato, Y. Inoue, Y. Ohtera, and S. Kawakami, "Cylindrical vector laser beam generated by the use of a photonic crystal mirror," Appl. Phys. Express **1**(2), 022008 (2008).
17. M. A. Ahmed, J. Schulz, A. Voss, O. Parriaux, J.-C. Pommier, and T. Graf, "Radially polarized 3 kW beam from a CO2 laser with an intracavity resonant grating mirror," Opt. Lett. **32**(13), 1824–1826 (2007).
18. M. Rumpel, M. Haefner, T. Schoder, C. Pruss, A. Voss, W. Osten, M. A. Ahmed, and T. Graf, "Circular grating waveguide structures for intracavity generation of azimuthal polarization in a thin-disk laser," Opt. Lett. **37**(10), 1763–1765 (2012).
19. M. A. Ahmed, M. Haefner, M. Vogel, C. Pruss, A. Voss, W. Osten, and T. Graf, "High-power radially polarized Yb: YAG thin-disk laser with high efficiency," Opt. Express **19**(6), 5093–5103 (2009).
20. J. W. Kim, J. I. Mackenzie, J. R. Hayes, and W. A. Clarkson, "High power Er:YAG laser with radially-polarized Laguerre-Gaussian (LG_{01}) mode output," Opt. Express **19**(15), 14526–14531 (2011).
21. M. Huonker, C. Schmitz, and A. Voss, "Laserverstaerkeranordnung," Europaeische Patentanmeldung, EP 1 178 579 A2, 2002.
22. M. Larionov, *Kontaktierung und Charakterisierung von Kristallen fuer Scheibenlaser* (Herbert Utz Verlag, 2009, Vol. 53).

1. Introduction

An optimized polarization distribution can significantly improve the absorption of the laser radiation during material processing. Theoretical and experimental studies have shown a considerable increase of the process efficiency, e.g. for drilling, cutting and deep-penetration welding, using cylindrically (radially or azimuthally) polarized laser radiation as compared to other polarization states [1–3]. Additionally, such beams offer interesting focusing properties [4–7] which can be used for a variety of applications such as optical tweezers [8] or particle acceleration [9].

In the past decades, several extra-cavity [10–12] and intra-cavity [13–16] approaches have been reported to produce beams with cylindrical polarization states. In the first case, this can be achieved by converting linear (or circular) polarization into radial and/or azimuthal polarization e.g. by sub-wavelength metallic or dielectric gratings [10] as well as segmented wave plates [11, 12]. In the second case, cylindrical polarization can be generated directly in a laser resonator e.g. by introducing customized polarizing devices [13–16]. Grating waveguide mirrors (GWM) were used in our experiments to generate radially polarized radiation inside a thin-disk laser (TDL) cavity [17–19]. A GWM consists of a sub-wavelength diffraction grating (which is circular in our case) integrated into a highly reflective (HR) multilayer mirror. In the present case it replaces the standard HR end-mirror in an Yb:YAG thin-disk laser resonator.

A standard TDL pumping optics was used so far to excite the cylindrically polarized LG_{01} mode [17–19]. In this configuration, the homogeneous flattop (super-Gaussian) pump beam emerging from the end facet of a fiber coupled pump diode is repeatedly imaged onto the surface of the disk. Since the cylindrically polarized LG_{01} mode however by nature exhibits vanishing intensity in its center, the homogeneous flattop pumping distribution has the disadvantage of

#248339 Received 21 Aug 2015; revised 15 Sep 2015; accepted 15 Sep 2015; published 1 Oct 2015

a reduced extraction efficiency in the center of the pump spot. The deposited pump energy is therefore lost as thermal energy and has to be dissipated via the cooling heat sink. In fact, the resulting strong temperature increase in the center can cause damage to the disk and has limited previous experiments [18]. In order to mitigate this issue, we have investigated various approaches to pump the thin-disks with a ring-shaped intensity distribution. The performance of the thereby pumped thin-disk lasers are compared to the one of common thin-disk lasers with a flattop pumping scheme. We show that using ring-shaped pumping leads to a significant reduction of the temperature (i.e by approximately 21%) in the central area of the disk while keeping the laser efficiency as high as in the case of the flattop pumping (i.e around 41% at an output power higher than 100 W).

2. Generation of ring-shaped pumping distributions

The two approaches discussed in the following are both based on the use of fiber capillaries as shown in Fig. 1. In one case, the beam shaping is performed by coupling the pump radiation into the wall of a simple cylindrical hollow fiber (see Fig. 1(a)) with the length L_a and the outer and inner diameters D_O and D_I, respectively. With this approach the incident pump beam needs to be focused to a diameter smaller than the wall thickness $(D_O - D_I)/2$ of the hollow fiber. Kim et al. have demonstrated a similar concept for an Er:YAG bulk laser yielding 13.1 W of radial polarized continuous wave output at a wavelength of 1645 nm [20].

In a further approach the hollow fiber capillary was collapsed on the side were the pump radiation is incident (see Fig. 1(b)). Here the fiber is collapsed to a cylindrical volume with diameter D_F over the length L_b. The focus of the incident pump beam now should be smaller than D_F, which is larger than $(D_O - D_I)/2$. The length of the conical part is L_c. In this conical part the inner diameter increases linearly from zero to D_I, whereas the outer diameter increases linearly from D_F to D_O. The shaped beam exits the capillary on this side (right of Fig. 1(b)).

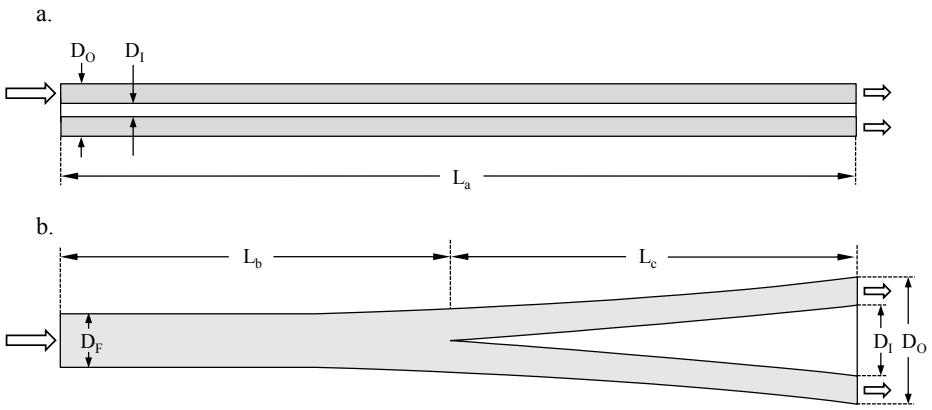

Fig. 1. Sketch of the geometry of the used hollow beam-shaping fibers; a) hollow capillary and b) collapsed capillary.

An optical system composed of two biconvex BK7 lenses with a focal length of 15 mm and a diameter of 12.7 mm were designed and used to launch the fiber-coupled pump radiation (fiber with core diameter of 600 μm and NA = 0.22) with a wavelength of 940 nm into the beam shaping fibers.

In order to achieve efficient laser operation, an optimum overlap between the pump light distribution and the laser mode is required. In a first step this was investigated theoretically by analyzing the intensity distribution generated by the two fiber geometries listed in table 1 with

#248339 Received 21 Aug 2015; revised 15 Sep 2015; accepted 15 Sep 2015; published 1 Oct 2015

the help of a commercial ray tracing software. The comparison of the calculated pump intensity distributions generated by the two fiber-optic beam shaper and the LG_{01} laser mode is shown in Fig. 2.

Table 1. Geometrical parameters for the simulation of the hollow capillary (first row) and the collapsed fiber capillary (second row) with the same diameter ratio D_I/D_O.

	D_O	D_I	D_I/D_O	L_a	L_b	L_c
Hollow capillary	1434 μm	343 μm	0.239	565 mm	-	-
Collapsed fiber	1434 μm	343 μm	0.239	-	80 mm	485 mm

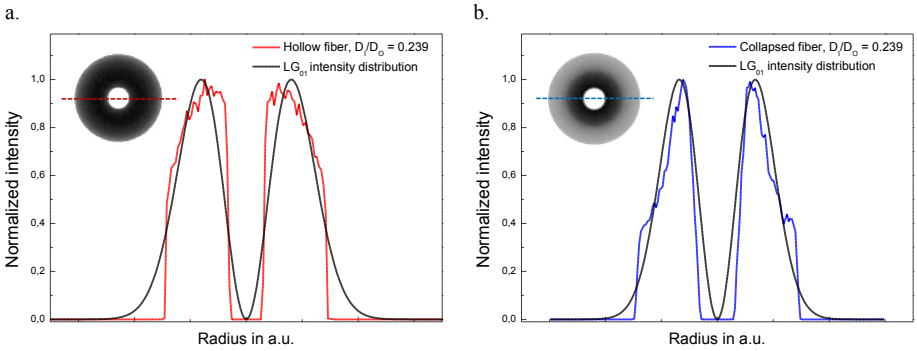

Fig. 2. Comparison between the oscillating ring mode (black line) and the ring-shaped intensity distribution generated by the hollow capillary (a.) and the collapsed fiber (b.).

As can be seen from the two cross sections, the hollow fiber geometry exhibits a more homogeneous distribution of the intensity within the ring profile with a moderate increase of the intensity towards the inner diameter of the profile (Fig. 2(a)). With the geometry given in table 1 the intensity distribution produced by the collapsed fiber (Fig. 2(b)) exhibits a more pronounced maximum at the inner side. Longer fibers would most likely lead to a more uniform distribution of the intensity. To find and to compare the achievable overlap

$$F = 1 - \frac{\int \left| I_{Pumpspot} - I_{Ringmode} \right|}{\int I_{Pumpspot}} \tag{1}$$

of the LG_{01} ring mode and the (calculated) pump intensity profiles produced by the two fiber-optic beam shapers, an optimization algorithm was used that varied the diameter of the LG_{01} ring mode (corresponding to an adaptation of the laser resonator later in the experiments) to maximize the overlap. No saturation effects were taken into account by this approach. The calculation does also not consider additional smoothing of the intensity that might occur during the multiple re-imaging of the pump beam on the laser disk by the thin-disk laser pumping scheme. The maximum achievable overlap of a flattop pump distribution and the LG_{01} mode was calculated to be 55.05%. For the collapsed fiber the maximum achievable overlap was found to be F = 70.10%. Thanks to the slightly more homogeneous distribution, the hollow capillary leads to a slightly higher geometrical matching with F = 73.46%. Based on this result it was decided to use the hollow capillary approach for the further experimental investigation.

#248339 Received 21 Aug 2015; revised 15 Sep 2015; accepted 15 Sep 2015; published 1 Oct 2015

3. Experimental set-up

The set-up of the ring-pumped radially polarized thin-disk laser is schematically shown in Fig. 3. A fiber-coupled pump diode with a maximum output power of $P_{pump} = 418$ W at a wavelength of $\lambda = 940$ nm was used to pump the Yb:YAG disk, which had a thickness of 130 μm and a doping concentration of about 11%. The laser crystal was glued on a water cooled diamond heat sink for efficient heat extraction. It is AR-coated on the front surface and HR-coated on the back surface for both the pump and the laser wavelength at 940 nm and 1030 nm, respectively. The radius of curvature of the mounted disk was R = 2.1 m. A standard 24-passes B1 pumping module (as available from the IFSW) was used to ensure a sufficient absorption of the pump radiation in the thin-disk crystal. The laser resonator was designed for a beam propagation factor of $M^2 = 2$ as given by the LG_{01} mode. It comprises a plane output coupler (OC) with a transmission of 4%. A telescope composed of a 800 mm concave mirror and a 500 mm convex mirror is implemented to adapt the size of the ring mode on the disk. Additionally this leads to a collimated beam between the disk and the GWM and therefore minimizes the power density on the GWM. The GWM is used as the plane end-mirror of the resonator.

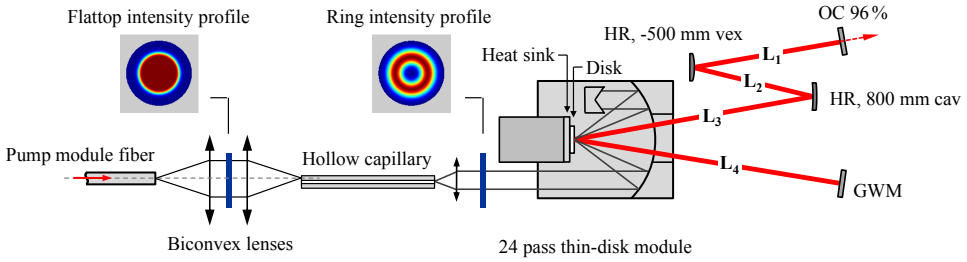

Fig. 3. Experimental setup for the LG_{01} mode Yb:YAG laser resonator.

The GWM is based on the leaky-mode coupling mechanism which allows sufficient reduction of the reflectivity of the polarization state to be suppressed in the resonator. More details about this kind of structures, including their modeling and fabrication, can be found in [17–19]. The measured spectral properties of the circular GWM are shown in Fig. 4.

The noticeable reduction of the reflectivity for the TE polarized light (corresponding to azimuthal polarization with a circular grating) is adequately well centered at the laser wavelength of the Yb:YAG at $\lambda = 1030$ nm and leads to the effective suppression of the azimuthally polarized modes in the resonator. As the reflectivity for the TM polarized light is virtually unaffected by the presence of the grating this leads to the efficient generation of pure radially polarized modes. The absolute reflectivities for the TE and TM polarized probe beams were measured to be $(94 \pm 0.3)\%$ and $(99.7 \pm 0.3)\%$, respectively, which corresponds to a reflectivity difference of $\Delta R_{TM-TE} \approx 5.7\%$ at the central wavelength of the Yb:YAG thin-disk laser i.e. 1030 nm.

Before implementing different fiber components into the pump beam path, reference measurements were made with the commonly used flattop pumping distribution. The distances of the resonator arms L_1, L_2, L_3 and L_4 were set to be 155 mm, 140 mm, 315 mm and 300 mm, respectively. The pump spot diameter on the disk was 2.4 mm. A maximum output power of 116.7 W at a pump power of 279.4 W - which corresponds to an optical efficiency of $\eta_{opt.} = 41.7\%$ - was achieved generating a radially polarized ring mode with a measured beam propagation factor of $M^2 \approx 2.3$. The efficiency of the laser is lower than expected and can be essentially attributed to the additional intra-cavity losses introduced by the GWM since its reflectivity (99.5%) is lower than that of a standard HR (99.99%) mirror. Furthermore depolarization losses in the range of 0.1-0.3% per round-trip contribute to lowering of the laser performances.

#248339 Received 21 Aug 2015; revised 15 Sep 2015; accepted 15 Sep 2015; published 1 Oct 2015

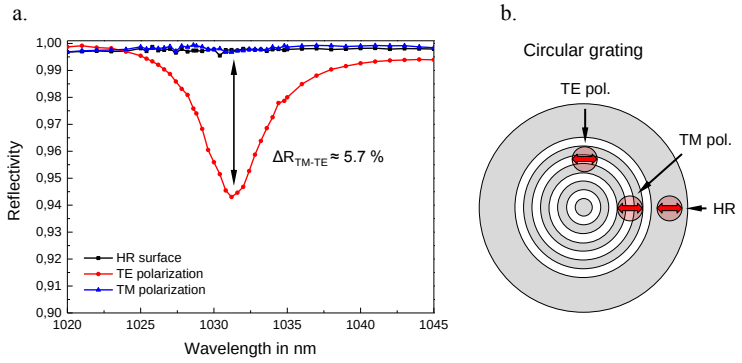

Fig. 4. Wavelength dependence of the spectral reflectivity distribution for TE and TM polarization at normal incidence (a). The reflectivity of the GWM was measured by a probe beam collimated on the structured surface with the circular grating as sketched on the right hand side (b). The orientation of the probe beams polarization is indicated by the red arrow. The reflectivity of the original HR coating was measured by probing the mirror surface outside the structured area.

For the investigations of the laser performance with ring-shaped pumping and to be able to test different aspect ratios of the pumped area on the laser disk, four different hollow capillary geometries with a length of 300 mm were manufactured using our fiber drawing tower. As the (outer) diameter of the resulting pump spots on the disk slightly varied between 2.3 mm and 2.4 mm for the different capillaries, the resonator was adapted by changing the lengths L_1 and L_2 as appropriate to ensure maximum achievable optical efficiency and a pure LG_{01} ring mode oscillation over the whole pump power range. Table 2 lists all tested fibers with the corresponding resonator lengths L_1 and L_2, the mode diameter $d_{LG_{01}}$ on the disk as well as the total resonator length $L_{Tot.}$ and the calculated overlap F.

Table 2. Geometrical parameters used for the experimental comparison of the performance of the radially polarized laser with flattop and ring-shaped pumping.

Pumping	D_I	D_O	D_I/D_O	L_1	L_2	$d_{LG_{01}}$	$L_{Tot.}$	F
Flattop	-	-	-	155 mm	140 mm	2.43 mm	910 mm	55.05%
Cap. #1	290 μm	1300 μm	0.225	145 mm	130 mm	2.25 mm	890 mm	68.38%
Cap. #2	247 μm	1300 μm	0.188	145 mm	130 mm	2.25 mm	890 mm	68.82%
Cap. #3	193 μm	1284 μm	0.147	130 mm	130 mm	2.15 mm	875 mm	70.02%
Cap. #4	172 μm	1304 μm	0.125	145 mm	130 mm	2.25 mm	890 mm	70.39%

The coupling efficiency of the beam shaping fiber was measured to be in the range of 78% to 80%. For the following comparison of the laser performances achieved with flattop and ring-shaped pumping we always refer to the pump power P_{pump} incident at the thin-disk module.

4. Thin-disk laser performance

With the hollow capillary #1 ($D_2/D_1 = 0.225$), see tab. 2, an output power of 90 W was achieved at a pump power of 235 W incident at the thin-disk pumping module. This corresponds to an optical efficiency of $\eta_{opt.} = 38.3\%$. With the capillaries #2 ($D_2/D_1 = 0.188$) and #3 ($D_2/D_1 = 0.147$), the optical efficiencies at the maximum power were measured to be 39.9% and 40.2%, respectively. The best performance with an output power of 107 W at a pump power of 260 W

#248339 Received 21 Aug 2015; revised 15 Sep 2015; accepted 15 Sep 2015; published 1 Oct 2015

incident at the thin-disk pumping module was achieved with the hollow capillary #4 (D_2/D_1 = 0.125). This corresponds to an optical efficiency of $\eta_{opt.}$ = 41.2%.

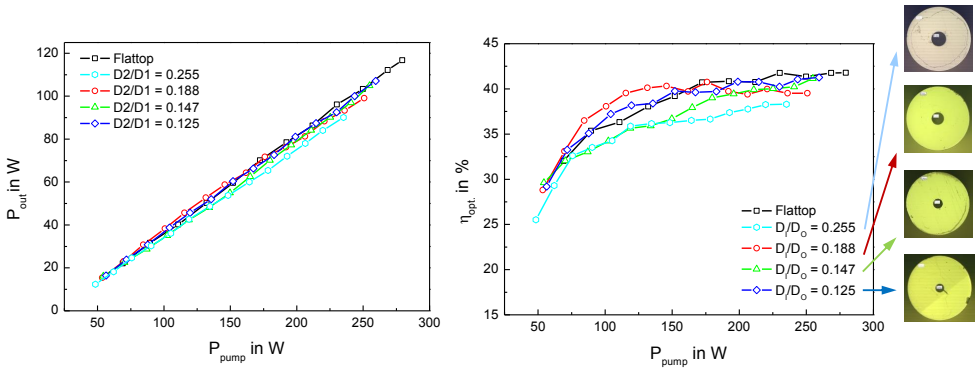

Fig. 5. Output power (left) and optical efficiency (right) of the radially polarized thin-disk lases pumped either by a flattop or by ring-shaped pumping distribution as generated by the fiber-optic beam shaper (whose cross-sections are shown on the very right).

In these experiments the applicable pump power was limited by the stability range of the resonator (in both flattop and ring pumping schemes) which was designed to support the LG_{01}-mode with the desired large diameter of 2.3 to 2.4 mm. Figure 5 summarizes the output powers and the optical efficiencies of the lasers pumped with the different pumping distributions. In all experiments the M^2 value was measured to be around 2 at all power levels, which is consistent with generation of the radially polarized LG_{01} mode.

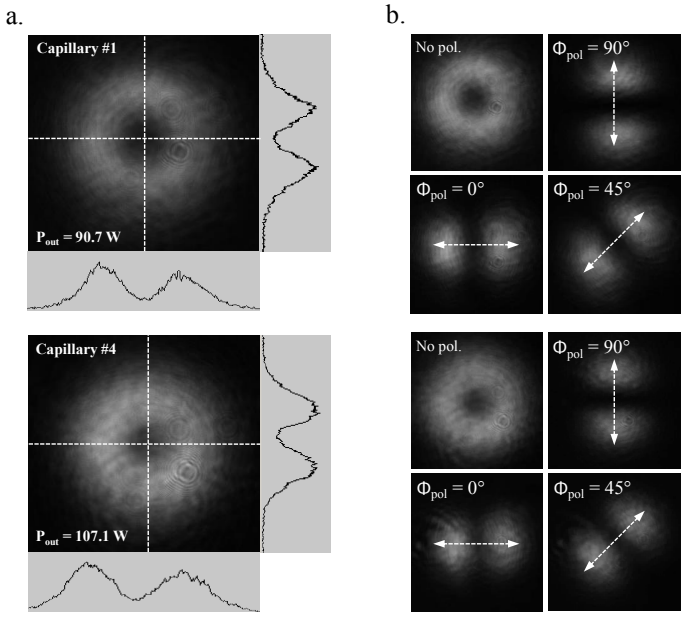

Fig. 6. Far field intensity distribution of the output beam (a.) as generated by the laser pumped through capillary #4 and analysis of its polarization distribution as transmitted through a rotating linear polarizer (b.).

#248339 Received 21 Aug 2015; revised 15 Sep 2015; accepted 15 Sep 2015; published 1 Oct 2015

As can be seen the difference between the laser performances using the 4 different capillaries is comparably small but agrees well compared to the change of corresponding values of the calculated mode overlap given in tab. 2. Further investigations will require a more comprehensive simulation considering additional phenomenon such as laser saturation and will be subject of future studies. The intensity distributions of the output beam generated by the laser pumped through capillary #1 and capillary #4 are shown in Fig. 6(a). Figure 6(b) shows the qualitative analysis of the polarization of the beams by recording their intensity distributions transmitted through a rotating polarizer which confirms the radial polarization of the LG_{01} output beam.

The results discussed so far show that a radially polarized LG_{01} mode can be generated by means of a ring-shaped pump beam distribution with at least the same efficiency as obtained by pumping with a flattop distributed pump beam profile. The most significant difference is evident from Fig. 7 which shows the fluorescence distribution emitted by the thin-disk laser crystal during laser operation in the LG_{01} mode.

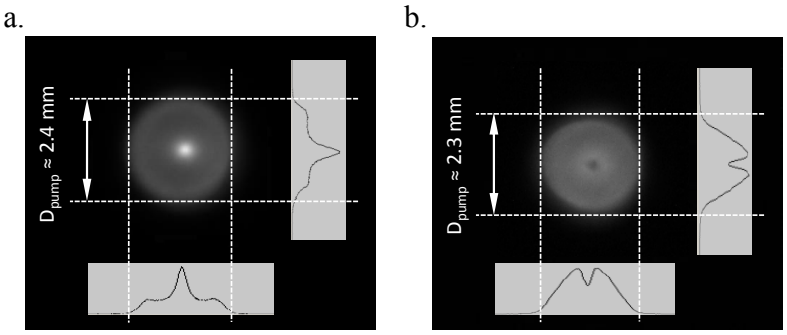

Fig. 7. Distribution of the fluorescence emitted from the thin-disk laser crystal either homogeneously pumped by a flattop pumping distribution (a) or by the ring-shaped distribution produced by capillary #4.

In the left-hand picture (Fig. 7(a)) one clearly notes the excessive fluorescence caused by the non-saturated excitation in the center of the homogeneously pumped disk, which leads to strong heating of the crystal as discussed in the next section. As seen from Fig. 7(b) this considerable heating source is avoided in the case of the ring-shaped pumping.

5. Temperature distribution across the thin-disk laser crystal

An IR thermo camera (IRBIS VarioCAM) was used to monitor the temperature distribution on the front surface of the thin-disk laser crystal. Due to its limited spatial resolution the thermo camera was placed at a distance of 150 mm from the crystal which allowed to resolve the pump spot diameter with about 30 pixels. A cross-section of the temperature profile over the radial position at a pump power of 225 W is shown in Fig. 8(a). Furthermore, the measured increase of the temperature during laser operation with increasing pump power is summarized in Fig. 8(b).

For a pump power of 225 W, a maximum temperature of 82.5°C is measured in the center of the flattop pumped spot (pos. (a) in Fig. 8(b)). Using the ring-shaped pumping distribution leads to a maximum temperature in the center of the pumping area of about 68.9°C (pos. (b) in Fig. 8(b)). This corresponds to a temperature difference of ΔT_{center} = 13.6°C.

At a higher pump power of 280 W the maximum temperature in the center of the flattop shaped pump spot reached 100.7°C, which corresponds to a temperature increase of ΔT = 85.7°C with respect to the starting temperature of the crystal at 15°C as given by the cooling

#248339 Received 21 Aug 2015; revised 15 Sep 2015; accepted 15 Sep 2015; published 1 Oct 2015

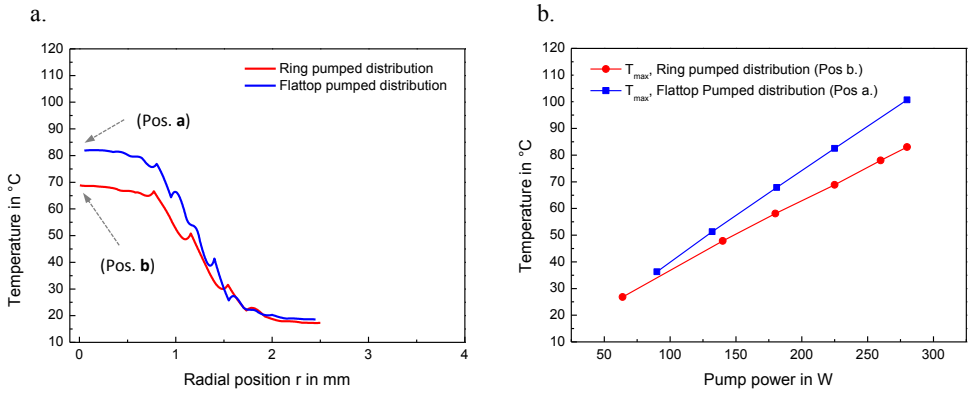

Fig. 8. Cross-section of the temperature measurement on the front surface of the thin-disk laser crystal for a pump power of 225 W (a) and comparison of the measured temperatures as a function of the pump power measured at pos. a and pos. b (b).

mount. With 280 W of power in the ring-shaped pumping distribution the maximum temperature in the center of the crystal was only 83.0°C, which corresponds to a temperature increase of $\Delta T = 68$°C. This means that the temperature increase of the crystal is reduced by 21% when pumped with the appropriate ring-shaped distribution.

6. Conclusion

In summary, we have shown the potential of ring-shaped pumping distributions for the generation of LG_{01} modes in high-power thin-disk laser. A beam with radial polarization with a maximum output power of 107 W and an optical efficiency of 41.2% was demonstrated using a GWM in the resonator and a glass capillary to shape the pump beam into a ring-shaped intensity distribution. To the best of our knowledge this is the first demonstration of a radially polarized thin-disk laser using ring-shaped pumping. The measured optical efficiency of the laser was shown to be comparable to that with a flattop pump beam.

The main advantage of the ring-shaped pumping distribution was found to be the reduction of the temperature increase on the disk surface of about 21% (at 280 W of pump power). This should allow higher pump power densities without increasing the risk of damaging the disk or distorting the polarization purity.

Acknowledgments

This work is partly supported by the Ultrafast_RAZipol project funded by the European Unions Seventh Frame-Work Program for research, technological development, and demonstration under grant agreement no. 619237. In addition, this work was supported by the German Research Foundation (DFG) within the funding program Open Access Publishing.